ELSEVIER

Contents lists available at ScienceDirect

Materials Today Communications

journal homepage: www.elsevier.com/locate/mtcomm





An atomistic study of deformation mechanisms in metal matrix nanocomposite materials

Md Shahrier Hasan, Gregory Berkeley, Kyrel Polifrone, Wenwu Xu

Department of Mechanical Engineering, College of Engineering, San Diego State University, San Diego, CA 92182, United States

ARTICLE INFO

Keywords:
Molecular dynamics
Metal matrix nanocomposites
Al-SiC
Deformation mechanisms
Dislocations

ABSTRACT

With nanoscale reinforcements resulting in a high density of matrix/reinforcer interfaces, metal matrix nano-composite (MMNC) materials behave differently from their micro-composite counterparts. An atomistic level understanding of the fundamental deformation mechanisms is necessary to link the nanoscale reinforcement attributes with the strengthening and fracture properties of the nanocomposite. Using the Aluminum-(Silicon Carbide), Al-SiC, nanocomposite as an example, we conducted classical Molecular Dynamics simulations of uniaxial tensile deformation for the composite. By varying nanocomposite design parameters, including the SiC particle size, and the particle volume fraction, we revealed the deformation mechanisms and defects evolution in nanocomposite materials. The deformation mechanisms are characterized into three subsequent mechanisms, which are (I) defect-free deformation driven by lattice distortion of the matrix, (II) dislocation-based deformation driven by dislocation nucleation and growth, and (III) failure-based deformation driven by interface separation and void growth. The nanoparticle volume fraction was found to have a major effect on dislocation-based deformation, whereas the particle size had a greater impact on the failure-based deformation. This work sheds light on the fundamental deformation mechanisms of MMNCs which may facilitate the future design of advanced nanocomposites with broader applications.

1. Introduction

With the emergence of composite technology for the weight critical application in engineering and biomedical sectors, metallic composites hold a great significance as metals are the most widely used class of materials in structural application. In the past few decades, conventional alloying techniques has improved capabilities of existing metals and produced materials like high performance steels with enhanced strength [1] or, nickel superalloys with great refractory properties [2]. Recently, high entropy alloys also generated great interest in the material science community attributed to their unique physical, chemical, and mechanical properties that are not found in the monolithic metals or conventional alloys [3]. However, the alloying property enhancement techniques are somewhat limited as the alloy's properties closely follow the properties of the base material. Metallic composites opens up an avenue to explore property space that are unattainable in available materials and alloys as the constituent particle in these materials can be different like ceramic (e.g., SiC, SiO2, Al2O3) or even non-metals like graphene sheets, carbon nanotubes, and so on [4].

The driving principle behind the design of metallic composites so far has been to combine the ductility and toughness of the metal matrix with the high stiffness and strengths of the particulate. The micron-sized particulate reinforced metallic composites, also known as metal matrix composites, MMCs, have been in used in the automotive, electronic packaging, and manufacture of golf club, bicycle, and so on [5]. Most of these MMC applications are weight critical in nature i.e., the reinforced composites are supposed to outperform other monolithic materials as a ratio of their weights to justify their applications. Since the weight penalty in MMCs are needed to be compensated by the property enhancement, it imposes limitation on the range of applications feasible for this class of materials. Moreover, the micron-sized reinforcement deteriorates some important mechanical properties like fracture toughness, formability, machinability and also tribological property of the composites [6].

Reducing the size of the reinforcing particulate to nanoscale has shown a great promise to mitigate some of the limitations of MMCs. With significantly lower volume fraction of reinforcing nanoparticle, disproportionately larger property enhancement is reported in the experiments

E-mail address: wenwu.xu@sdsu.edu (W. Xu).

^{*} Corresponding author.

[4]. This new class of materials, the so called metal matrix nano-composites (MMNCs), is also conducive to machining, since the nano-particulate cannot wear down the machining tools [7]. MMNCs also demonstrate isotropic property improvements even for non-spherical reinforcement as there are a large number of nano-particulates which average out any directionality [8]. However, with all these benefits over MMCs, the manufacture of MMNCs have proven to be more difficult. In particular, achieving a homogeneous dispersion of nanoparticles through-out the matrix has proven to be challenging.

Another great challenge for the application of MMNCs is the need for a novel design principle that is different from that of MMCs. As previously stated, the guiding principle for design of the MMCs involves combining the property of the matrix and particle to estimate the property of the composite. This method falls short for the MMNCs as there exists a significant portion of matrix/particle interface in the material systems. The atoms at the interfaces are energetically less stable due to the lattice mismatch and hence, more actively participate in the deformation under the mechanical loading. The well-established strengthening models of MMCs like the Rule of Mixture (ROM) or, Shear lag [9] are found to be unreliable for MMNCs. Also in MMCs, the failure is initiated mostly by the brittle fracture of the ceramic particle [10] unlike MMNCs where the nano-ceramic particle are unlikely to fracture and failure mechanism is a result of nano-voids generated from the matrix/particle interfaces and coalesced into micro-voids. Therefore, there is a need to understand the fundamental strengthening and failure mechanisms of MMNCs at the atomistic scale.

Several experimental investigations have been carried out to understand the strengthening mechanism of MMNCs with varying success. Goh et al. investigated the strengthening mechanism in Magnesia-Yttria, Mg-Y2O3, MMNC and found that the load bearing mechanism of strengthening to be secondary to the Orowan's dislocation bowing mechanism [11]. In some experimental studies, other factors like thermal coefficient mismatch, grain refinement, elastic modulus mismatch have also been reported to be the driving mechanism for MMNC strengthening [12,13]. Some studies emphasized the effect of refined grain size for the MMNC strengthening. This refined grain size in the MMNC exist as a result of nanoparticles restricting grain boundary migration during the solidification and grain growth process [14]. However, Ferguson et al. compared Mg based MMNC with the Mg alloy AZ31 with comparable grain-size and reported strengthening and loss of ductility in MMNC regardless of grain-refinement effect [15]. Several other experimental investigations on MMNC strengthening for varying particle-reinforcement have reported somewhat conflicting results. There are various reasons for these inconsistent experimental data, such as: difficulty to keep the nanoparticles contaminant free, agglomeration of nanoparticles, difficulty to obtain homogeneous dispersion which affects the mechanical property of MMNCs, larger scale micro-structure of the metal-matrix being different for different specimen adversely affecting the reproducibility of the experimental results.

Atomistic simulation technique is a computational tool for material scientists to uncover mechanisms in materials with atomistic details [16-18]. From understanding interfacial properties such as free energy [19], and wettability through first-principles calculations [20] to classical Molecular Dynamic (MD) simulation to discover high rate mechanisms [21], atomistic techniques are particularly suitable to understand MMNCs. The reason is that MMNCs involve nanoscale complexity where nanoscale mechanisms control the overall behavior of the materials. Classical MD simulation, even with its inherently limited scope in terms of time and space, can sufficiently describe the important mechanisms in MMNCs [22]. MD simulations can be more reliable than experimental observation as it does not suffer from the possibility of material contamination and inhomogeneous particle dispersion which may affect the experimental results. Hence, for an incisive investigation to uncover deformation mechanisms in MMNCs as a function of nanoparticle characteristics, MD simulation is a scale-appropriate tool.

Aluminum, Al, and its alloys are one of the most important and widely used metals in today's manufacturing industry. This relatively light metal has excellent ductility and formability. However, its bulk stiffness and strength is not comparable relative to its heavy metal counterparts like steel. Through precipitate hardening, the strength of Al can be vastly improved but at elevated temperature this improvement fades away as the precipitate moves in the Al matrix and coalesces. An alternate way of strengthening and stiffening of Al is particle reinforcement, typically using ceramics [1]. As one of the most commonly used MMNCs, Silicon carbide, SiC, nanoparticle reinforced Al composite is investigated in this study as a test case. The outline of this work is as such: description of MD simulation and analysis procedure in Section 2, discussions on the simulation results for varying particle size and particle volume fraction is the Section 3, and finally, conclusion and future research direction is discussed in Section 4.

2. Methodology

2.1. Atomistic simulation method

To model the effect of Al-SiC nano-interface, all other form of nanointerfaces such as grain boundaries were excluded from the model. A major challenge for the synthesis of the nanocomposites remains achieving homogenous dispersion of nano-reinforcements in the matrix. Inhomogeneous dispersion and alignment of the nanoparticles lead to agglomeration that can severely affect the performance of the nanocomposites. Several experimental works have successfully developed and applied material synthesis methodologies to achieve homogeneous dispersion of the nanoparticles [23,24] in nanocomposites. This is still an active area of research for the development of nanocomposite with high performances. However, to focus on the effects of particle attributes on the mechanical properties and deformation mechanisms, the material synthesis problems such as particle agglomeration are not considered in the present work. In this work, a perfectly homogeneous dispersion of nanoparticles is assumed in our MD simulations. Also, the effect of particle alignment is neglected by assuming perfectly spherical SiC

Firstly, a series of atomistic models comprising single crystal Al matrix with a spherical SiC nanoparticle embedded in them were created with the Atomsk software tool [25]. The dimension of the Al matrix and the diameter of the SiC nanoparticle were parameterized based on desired particle density and specific surface of the nano-interface. The diameter of the nanoparticle was varied from 2 nm at the smallest to 7 nm at the largest while density of particle was varied from 0.5 % volume fraction to 4.5 % volume fraction based on reported experimental data [26]. The largest model had about 2 million atoms while the smallest model had about 44 thousand atoms. For the atomistic model of SiC nanoparticle, beta modification (β -SiC) of the polytypes were used which has a zinc-blende crystal structure that is stable at room temperature. To understand the alternative failure mechanism due to nano-reinforcement and compare with the mechanism in pure matrix, atomistic model of pure metal Al is also created.

A widely cited Embedded Atom Method (EAM) based potential function developed by Mishin et al. [27] is used in this work to model the interatomic interactions of Al atoms. The covalent bonds of zinc-blende SiC crystal are modeled with the Tersoff potential [28]. The nano-interface property is dependent on two body interactions of Al-Si and Al-C, and three body interactions of Al-Si-C, Al-C-Si, Al-Si-Al and Al-C-Al. However, for computational efficiency only two body interaction is considered which is modeled by a two-body pairwise Morse potential with parameters obtained from the work of Dandekar [29]. A large-scale atomic/molecular massively parallel simulation (LAMMPS) [30] is used to simulate the uniaxial tension condition on the atomistic models of Al-SiC nanocomposites along the X direction. No loading is applied in the Z direction which emulates plane strain loading condition of the continuum model. Periodic Boundary Condition (PBC) is applied

in all directions. The models are first relaxed at 300 K temperature and 1 bar pressure with the isothermal-isobaric (NPT) ensemble. To obtain equilibrium configuration, 100 pico-second (ps) is sufficient for the model with the largest amount of particle/matrix interface. Deformation is then applied at a strain rate of $5 \times 10^8/s$ at 300 K temperature and isothermal isochoric (NVT) ensemble.

2.2. Structure identification and dislocation quantification

A widely used MD simulation post-processing tool Open Visualization Tool (OVITO) [31] is used to analyze the simulation data. Common Neighbor Analysis (CNA) is a tool in OVITO that identifies local crystal structure by employing high dimensional signature to various arrangement of atoms. To analyze the data of present sets of simulations, adaptive CNA with a varying cut off radius which is particularly suitable for analyzing multi-phase systems [32]. In OVITO, Dislocation Extraction Algorithm (DXA) [33] is implemented which identifies isolated discrete dislocation core and Burgers vector by running recurrent Burgers circuit algorithm. Dislocation cores have a drastically different local coordination number than the defect-free lattice. Burgers vectors and dislocation lengths are identified, and dislocation lines are represented by line segments. This method is used on the entire MD simulation data to analyze crystal structure and identify the total dislocation line at each strain state. Finally, dislocation density is quantified by dividing the total number of dislocations with the instantaneous cell volume.

3. Results and discussions

The MD simulation of uniaxial tension was performed under the free strain condition as opposed to the free stress condition used for tensile simulation of nanowire [34] where the PBC boundary in the orthogonal direction is maintained at zero stress to imitate a free surface. The free strain condition used in the present work is appropriate for simulating an internal volume without the free surface effect.

The results of the tensile simulations of Al-SiC nanocomposite revealed several distinct deformation mechanisms depending on the particle size and volume fraction of SiC. For example, Figs. 1 and 2 presents a typical characterization of the tensile deformation behavior in the Al-SiC MMNC with a radius of 2 nm SiC particle and 2.5 vol% volume fraction. The overall deformation of the nanocomposite model can be split into 3 sequential regions signifying their respective deformation mechanisms, as indicated in Fig. 2. They are defect-free region (I), dislocation nucleation and growth region (II), and particle/matrix interface separation region (III).

In region I, strain is accommodated through lattice distortion which is not completely elastic due to the existing material's non-homogeneity. In this deformation mechanism, some bond breaking and atomistic realignment at the SiC particle/Al matrix interface takes place during load-transfer which adds some non-linearity in the stress response. As the stress response reaches its peak, defect-free lattice distortion can no

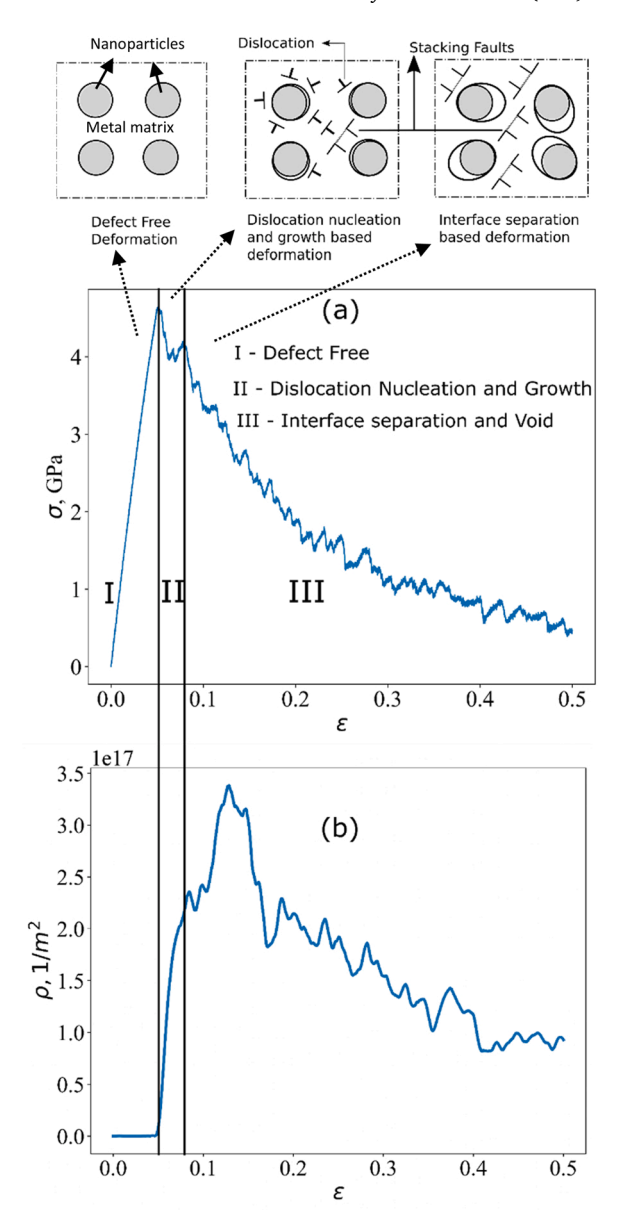


Fig. 2. Characterization of typical deformation mechanisms in Al-SiC nanocomposite with a radius of 2 nm SiC particle and a volume fraction of 2.5 vol%: (a) stress-strain curve; (b) dislocation density.

longer accommodate the additional strain. Instead of continuing building up, the stress is released by means of dislocation nucleation and growth, which corresponds to the region II. As shown in Fig. 2(b), the

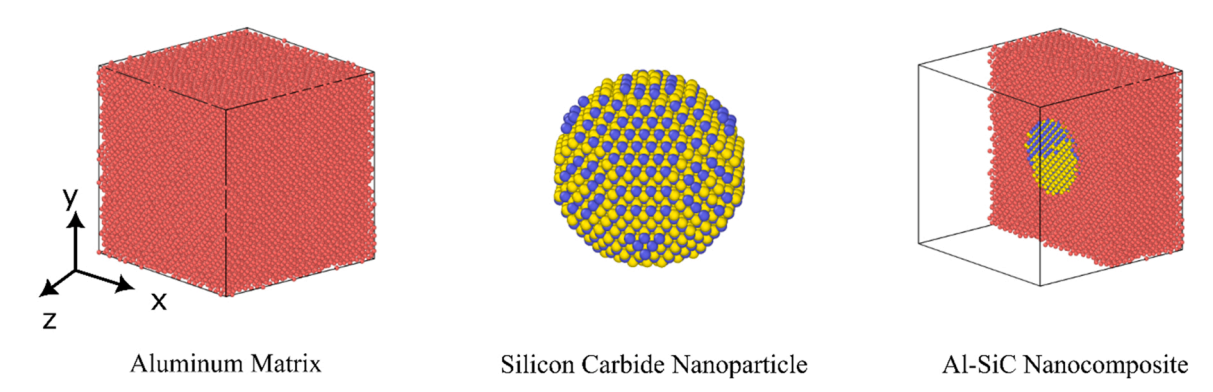


Fig. 1. Atomistic models of the FCC single-crystal Al (left), Zinc-Blende structured SiC nanoparticle (middle), and their composite (right).

computed dislocation density curve shows no dislocation in the defect-free region I, but as the nanocomposite is deformed beyond the defect-free region, a steady increase in dislocation density occurs, defining the dislocation nucleation and growth region II. From the stress-strain curve in Fig. 2(a), it can be observed that the stress response in region II decreases first, then stabilizes at a certain stress level below the region I's peak stress. In other words, the deformation in region II is primarily accommodated by the nucleation, growth, and motion of dislocations, thus, no obvious stress built-up occurs in response to deformation.

Upon application of further deformation (region III), stress response starts to progressively decrease (Fig. 2a). In the meantime, the overall dislocation density continues to climb up until a peak value is reached, then, decreases with further deformation modeling until a strain of ε = 0.5 in reached in our modeling. Note that, in region III, there are clear fluctuations of dislocation density values as the overall trend of the dislocation density is increased and then decreased. The increase and decrease trend in the dislocation density values in region III is found to be correlated with the particle/matrix interface separation and the void growth, respectively. The representative atomistic structural evolutions during the deformation will be provided in Fig. 5. The increase of dislocations in region III is due to the fact that the particle/matrix interfaces continue to act as the nucleation sites and generates more and more dislocation defects propagating in the metal matrix. The dislocation density reaches the peak value until the complete separation of the particle/matrix interface. After that, the voids start to form and grow, which corresponds to the overall decrease of dislocation density of region III. This reduction of dislocation density (i.e., $\varepsilon \gtrsim 0.14$ in Fig. 2b) is due to the dislocation annihilation at the free surfaces of the formed voids. Further deformation should result in the further growth of the void until the complete failure of the matrix is reached.

The deformation behavior in Al-SiC nanocomposite outlined in Fig. 2 is expected to be influenced by the volume fraction of the SiC nanoparticles. To investigate this effect, the stress response and dislocation

density curves of the Al-SiC nanocomposites containing 2 nm radius and 0.5 vol% to 4.5 vol% of SiC reinforcements are plotted in Fig. 3. First, as highlighted and plotted in the insets at the top of Fig. 3, the peak stress, i. e., the peak value at the end of the defect-free deformation region I, apparently varies with the change of the volume fraction of SiC. Note that the exceptionally high stress values are due to the large strain rate used in our modeling which is typical for MD studies. In general, the peak stress values of the composite are lower at a higher volume fraction of SiC. The higher vol% of SiC nanoparticle in the composite offers higher density of matrix/particle interfaces. The matrix/particle interfaces act as the nucleation sites for dislocations during deformation. Once the threshold (or yield) stress value is reached, the dislocation will start to nucleate at the matrix/particle interfaces. A higher density of matrix/particle interfaces in the composites facilitates the dislocation nucleation, thus, less amount of stress is needed for the nanocomposite to yield. In other words, the peak stress at the end of region I deceases at a higher vol% of SiC nanoparticles in the nanocomposite.

Interestingly, there exists a maximum value in the peak values of the dislocation density with the increase of vol% of SiC nanoparticle in the nanocomposite, as shown by the top-right inset in Fig. 3. This can be explained in terms of dislocation generations and interactions. The dispersion distance (homogeneous in our modeling) between nanoparticles decreases with the increase of the volume fraction of nanoparticles. At a relatively low nanoparticle volume fraction (0.5–2.5 vol%), the generated dislocations can travel longer distances and interact with each other, resulting multiplications of dislocations. Thus, the peak value of dislocations is increased with the increase of nanoparticle volume fraction (<2.5 vol% , see top-right inset in Fig. 3). However, when the nanoparticles' volume fraction is sufficiently highly (>2.5 vol%), interactions and multiplications amongst dislocations are inadequate, resulting in the decreased peak value of dislocation density (>2.5 vol% , see top-right inset in Fig. 3).

Since the SiC nanoparticle size also has an effect on the deformation

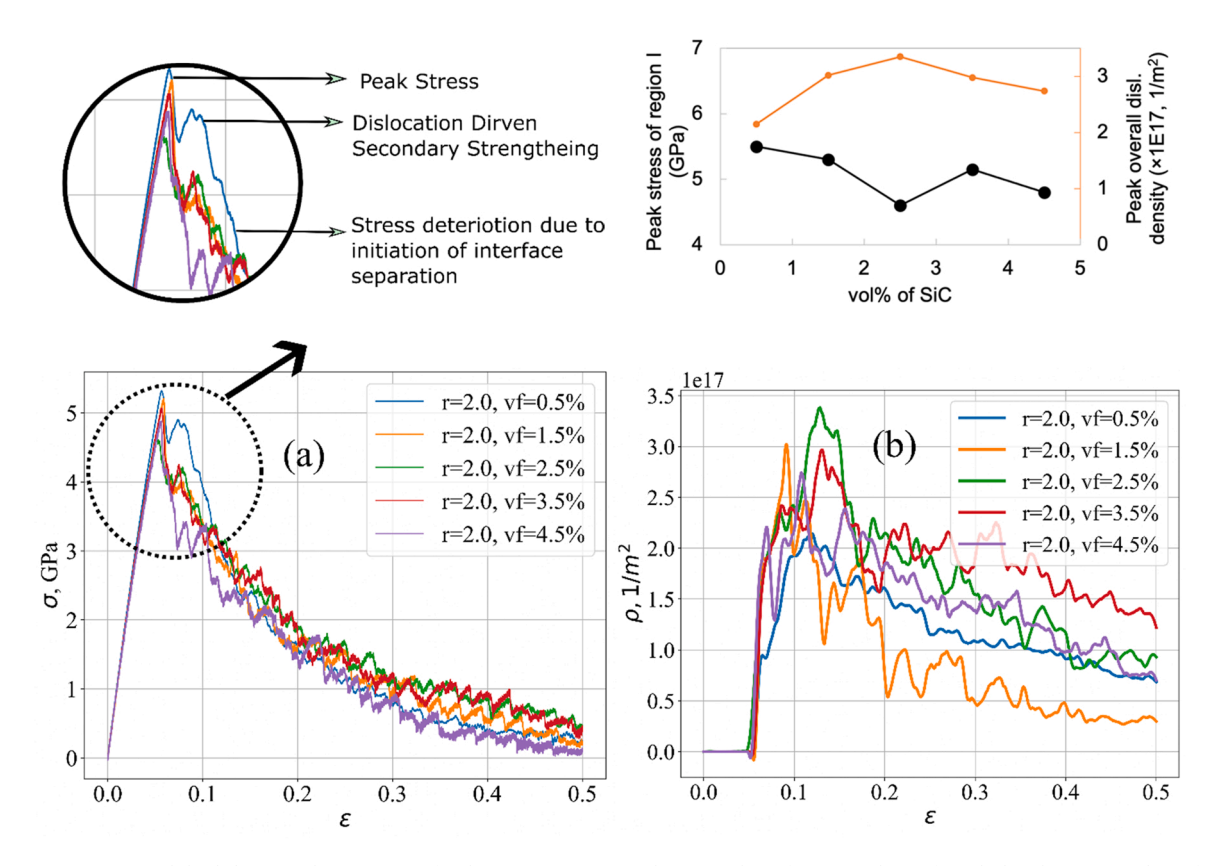


Fig. 3. (a) Stress response and (b) dislocation density curves for the nanocomposite with 2 nm radius of SiC particle reinforced Al with varying volume fraction from 0.5–4.5 vol%. Insets: local magnification of stress response (top left); summary of peak stress values as a function of SiC volume fraction (top right).

of Al-SiC nanocomposite, we investigated the SiC particle size dependence on the stress responses and dislocation densities, as the results shown in Fig. 4. As the nanoparticle radius increases from 2 nm to 7 nm, the specific surface of the spherical SiC nanoparticle reduces as follows,

Specific Surface
$$=$$
 $\frac{4\pi r^2}{\frac{4}{3}r^3} = \frac{3}{r}$ (1)

Since the specific surface of the nanoparticle is also the specific particle/matrix interface of the nanocomposite, particle radius inversely related to the strength of the interface. Hence, as the particle radius increases from 2-7 nm, interface strength progressively decreases. This is evident from Fig. 4(a) and the top-left local enlargement, the peak stress at the end of defect-free region I decreases with the increase of the radius of the SiC nanoparticle, signifying weaker interface that allows dislocation nucleation at a lower stress value. In the dislocation nucleation and growth region II, increasing particle size suppresses dislocation activity as can be observed from the dislocation density curve in Fig. 4(b) and the summarized peak dislocation values in the top-right inset. This is due to the relatively weaker interface which favors interface separation over dislocation nucleation as a deformation mechanism. Hence, the increased particle size accelerates the interface separation and the subsequent void growtssssh and ultimately failure of the nanocomposite.

Fig. 5(a) and (b) show the atomistic defect evolution as a mechanism of strain accommodation in the Al-SiC nanocomposite for SiC reinforcement of 2.5 % and 4.5 % volume fraction, respectively. Note that the matrix Al atoms with the perfect FCC structure are made invisible for clarity purpose. The general defect evolution corresponding to the previously stated deformation mechanisms can be explained as follows. In the defect free deformation, it can be observed that there are some point defects (vacancies and interstitials) as a result of lattice distortion and thermal fluctuations. After the peak stress is achieved, dislocation nucleation takes place that releases that accumulated stress during the

defect-free deformation. After the dislocation is nucleated, the dislocation will then grow and propagate to form a dislocation forest. Some of these dislocation splits into Shockley partials and form structures like stacking faults (SF). These stacking faults prevent dislocation propagation until dislocation propagation and growth can no longer sustain further deformation and interface separation becomes the primary mode of deformation mechanism.

As previously observed from the Fig. 3(b), enhancement of the dislocation activity due to the reinforcement is stagnated from 2.5 % volume fraction to 4.5 % volume fraction. This phenomenon can also be seen and understood directly from the atomic structure evolution in Fig. 5. As is shown that the dislocation forest growth is more readily interrupted by the neighborhood dislocation nucleation site as the SiC reinforcement volume fraction is increased from 2.5 % to 4.5 %. This interruption of dislocation forest growth leads to the premature formation of stacking faults, preventing dislocation propagation, and curtailing dislocation enhancement.

A direct comparison between experimental results and atomistic computation is problematic for several reasons. Firstly, the atomistic study in this work assumes a single crystal FCC matrix neglecting grain boundary effect. This assumption allows for an incisive analysis of the effect of the nanoparticle in the matrix and discovery of the underlying mechanism. But the mechanical properties obtained through experimental studies includes grain boundary effect and several studies reported grain-refinement based strengthening due to the nanoparticle reinforcement [35]. Secondly, the temporal constraint of MD simulation requires application of a very high strain-rate which only allows for the high-rate processes to occur. Thirdly, the size effect of the nanoparticles cannot be determined in an experimental set-up since nanoparticles sizes are usually determined through statistical average. Finally, in experiments, instead of pure metal Al, several Al alloys are used as matrix material because of their availability of well-documented base property values.

With these limitations under consideration, the mechanical

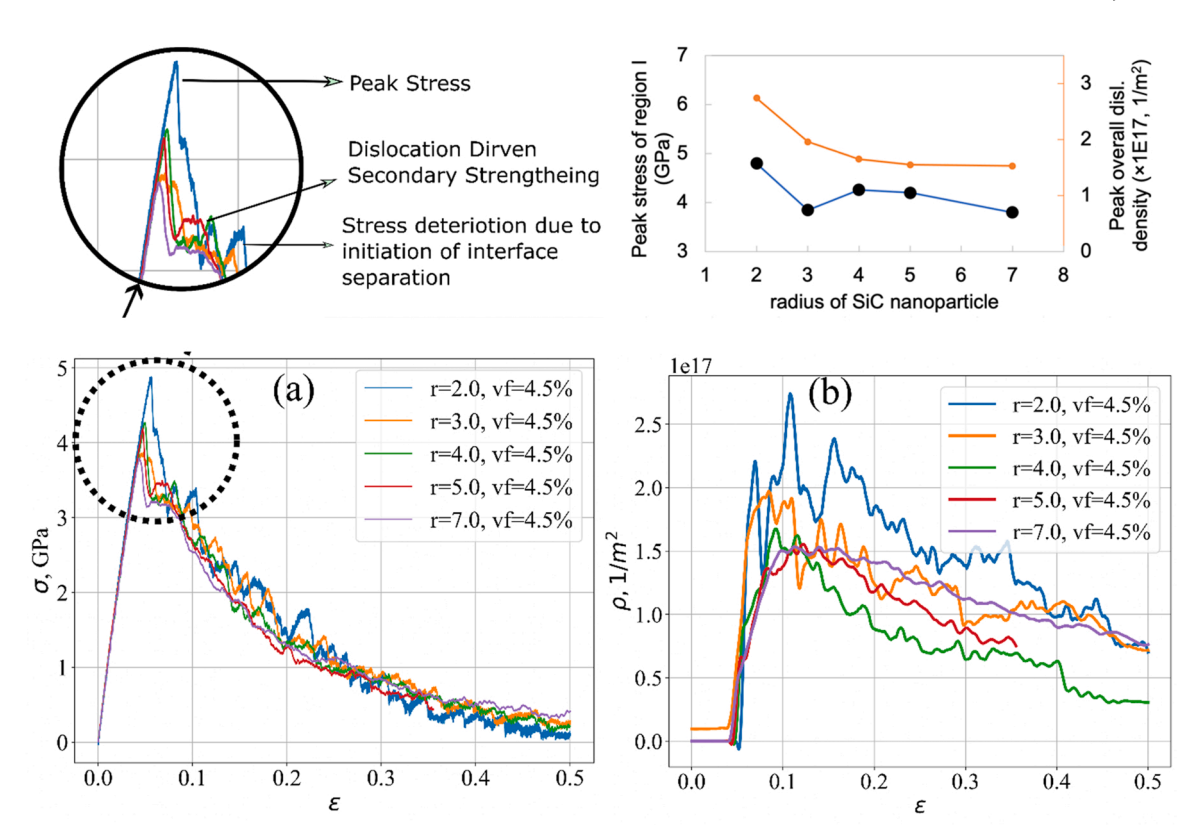


Fig. 4. Stress response (a) and dislocation density (b) curves of SiC particle of 2 nm to 7 nm reinforced in Al matrix at a 4.5 vol% volume fraction. Insets: local magnification of stress response (top left); summary of peak stress values as a function of size of SiC nanoparticles (top right).

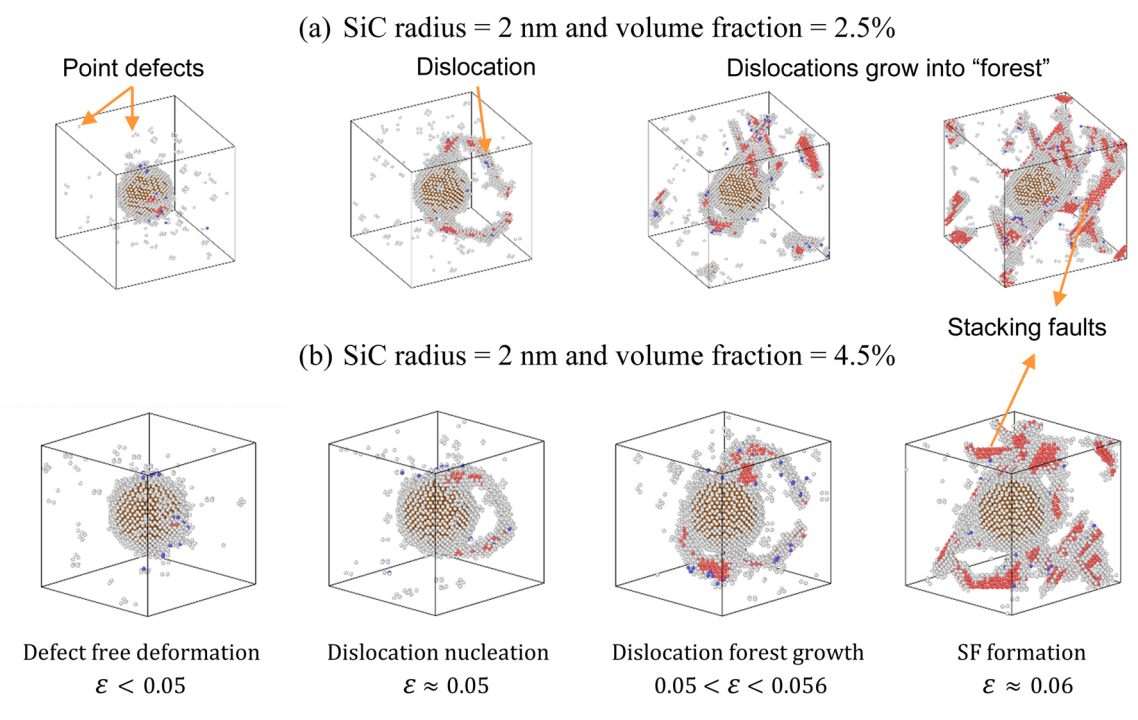


Fig. 5. Common Neighbor Analysis (CNA) of typical deformation mechanisms in the Al-SiC nanocomposite. Light grey atoms represent atoms in point (e.g., vacancies) and line (e.g., dislocations) defects. The red colored atoms represent the stacking faults that are created due to the split of full dislocation into Shockley partial dislocations.

properties of the Al-SiC nanocomposites recorded through several experimental works [36] can be attempted to be understood in light of the mechanism observed in the MD simulation of the present work. Fig. 6 demonstrates the mechanical properties of nano-SiC reinforced A356 matrix obtain by Mazahery et al. [26]. The nanocomposites were synthesized through two different processes, i.e., stir-casting and comp-casting. The nanocomposite prepared by the different synthesis root has different base properties but shows somewhat similar trend in response to the increase of SiC volume fraction. The experimental results show a very high sensitivity of mechanical properties of the nanocomposites to the nanoscale reinforcements of SiC particles. Indeed, the most dominant type of defect of the nanocomposites is the matrix-nanoparticle interface which controls the overall mechanical properties of the nanocomposites.

In case of ductility, there is a sharp decrease with the nano-SiC reinforcement at 0.5 vol% in A353 matrix. Increasing volume fraction of nano-SiC has minimal to no effect on ductility of the nanocomposite. To recall the atomistic deformation mechanism in Fig. 3, increasing particle volume fraction do not affect the deformation after the initiation of interface separation (region III in Fig. 2). The reason is that with the increasing particle volume fraction and similar particle size distribution, the interface strength remains unchanged. Since the interface separation and subsequent void growth remains the predominant failure mechanism, this explains that increasing nanoparticle volume fraction having no effect on ductility. Again, MD results in Fig. 3 revealed that increasing volume fraction of SiC nanoparticle enhances dislocation nucleation and growth which broadly explains the increasing hardness, yield tensile stress, and ultimate tensile stress as all of these properties are correlated to dislocation activity. MD results in Fig. 3(b) further shows that this dislocation enhancement has a taper-off effect at around 3.5 vol% reinforcement, or in other words, the dislocation contribution to the enhancement of strength of nanocomposite is curtailed. The experimental results of hardness, yield tensile strength and ultimate tensile strength in Fig. 6(b-d) also demonstrate similar taper off effect where the increase of SiC reinforcement above 3.5 % slow down property enhancement in the nanocomposite.

4. Conclusions

In this work, the atomistic deformation mechanisms in Al-SiC nanocomposite with varying size and volume fraction of SiC were systematically analyzed. Based on the MD simulation results, the following conclusions can be drawn:

- The reinforcement SiC nanoparticle volume fraction primarily influences the dislocation activity, which ultimately controls the properties like hardness, yield strength and ultimate strength of the material.
- 2. The size of the SiC particles affects the interface strength of the Al-SiC nanocomposite where increasing particle size weakens the particle/matrix interface. This interface separation being the primary mode of failure in Al-SiC nanocomposite, the size of SiC particle influences properties like ductility and fracture strength of the material.

The present study elucidates the atomistic mechanisms relevant for the deformation of Al-SiC nanocomposite as a function of SiC nanoparticle attributes' particle size and volume fraction. Particle volume fraction or the distribution density was found to influence the deformation mechanism that leads to strengthening. Particle size was observed to affect the deformation mechanism leading to the failure of the nanocomposite. Our fundamental understanding of atomistic deformation mechanisms in the Al-SiC nanocomposite is expected to provide guidance for a more targeted design of advanced MMNCs.

CRediT authorship contribution statement

Md Shahrier Hasan: Methodology, Investigation, Data curation, Writing – original draft. Gregory Berkeley: Methodology. Kyrel Poliforne: Investigation, Modify draft preparation. Wenwu Xu: Conceptualization, Supervision.

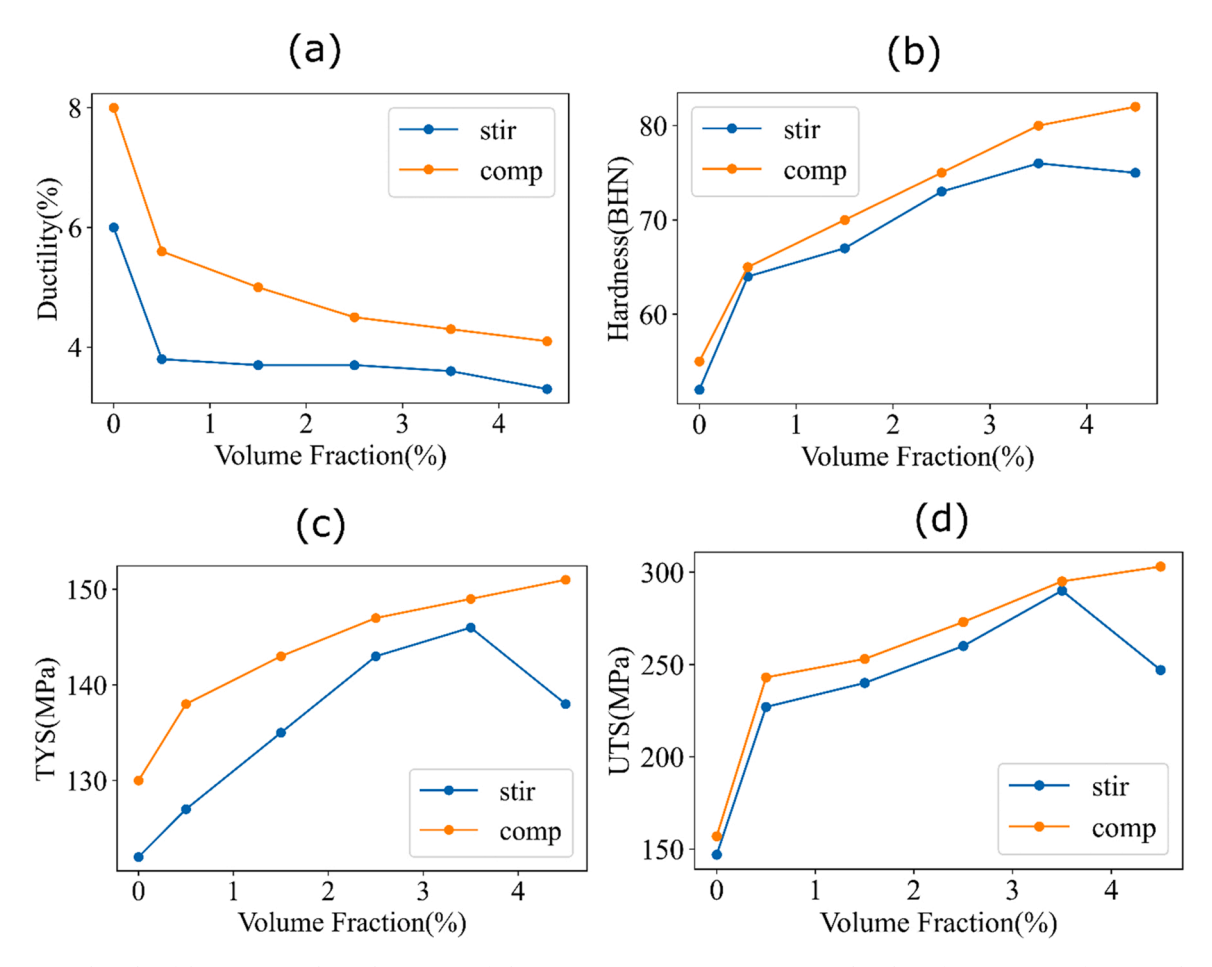


Fig. 6. Experimental results of the various mechanical properties of Al-SiC nanocomposites against nanoparticle volume fraction starting from 0.5 vol% to 4.5 vol% reinforcement [26]. Both stir-casting and comp-casting procedures were used to develop the Al-SiC nanocomposites, the following mechanical properties were measured (a) ductility, (b) hardness, (c) yield tensile strength (YTS), and (d) ultimate tensile strength (UTS).

Declaration of Competing Interest

The authors declare that they have no known competing financial interests or personal relationships that could have appeared to influence the work reported in this paper.

Data Availability

Data will be made available on request. The raw/processed data required to reproduce these findings cannot be shared at this time as the data also forms part of an ongoing study.

Acknowledgements

This work was performed under the support of the US National Science of Foundation, Division of Materials Research (Award No. 1900876) and the support of the US Department of Energy, Office of Basic Energy Sciences (Award No. SC0022244). The authors wish to thank the High-Performance Computing Cluster (HPCC) at SDSU for providing computing support for this project.

References

- [1] J.W. Kaczmar, K. Pietrzak, W. Włosiński, The production and application of metal matrix composite materials, J. Mater. Process. Technol. 106 (2000) 58–67, https:// doi.org/10.1016/s0924-0136(00)00639-7.
- [2] A. Thakur, S. Gangopadhyay, State-of-the-art in surface integrity in machining of nickel-based super alloys, Int. J. Mach. Tools Manuf. 100 (2016) 25–54, https:// doi.org/10.1016/j.ijmachtools.2015.10.001.

- W. Li, D. Xie, D. Li, Y. Zhang, Y. Gao, P.K. Liaw, Mechanical behavior of highentropy alloys, Prog. Mater. Sci. 118 (2021), 100777, https://doi.org/10.1016/j. pmateci 2021 100777
- [4] M. Malaki, W. Xu, A.K. Kasar, P.L. Menezes, H. Dieringa, R.S. Varma, M. Gupta, Advanced metal matrix nanocomposites, Metals 9 (2019) 330, https://doi.org/ 10.3390/met9030330
- [5] D.B. Miracle, Metal matrix composites from science to technological significance, Compos. Sci. Technol. 65 (2005) 2526–2540, https://doi.org/10.1016/j. compscitech.2005.05.027.
- [6] Y.-C. Kang, S.L.-I. Chan, Tensile properties of nanometric Al2O3 particulatereinforced aluminum matrix composites, Mater. Chem. Phys. 85 (2004) 438–443, https://doi.org/10.1016/j.matchemphys.2004.02.002.
- [7] R.L. Deuis, C. Subramanian, J.M. Yellup, Dry sliding wear of aluminium composites-a review, Compos. Sci. Technol. 57 (1997) 415–435, https://doi.org/ 10.1016/S0266-3538(96)00167-4.
- [8] A.I. Khdair, A. Fathy, Enhanced strength and ductility of Al-SiC nanocomposites synthesized by accumulative roll bonding, J. Mater. Res. Technol. 9 (2020) 478–489, https://doi.org/10.1016/j.jmrt.2019.10.077.
- [9] V.C. Nardone, K.M. Prewo, On the strength of discontinuous silicon carbide reinforced aluminum composites, Scr. Metall. 20 (1986) 43–48, https://doi.org/ 10.1016/0036-9748(86)90210-3.
- [10] M. Besterci, M. Garafa, M. Šlesár, G. Jangg, The influence of loading parameters on the deformation of the Al•Al4C3 system, Scr. Metall. Mater. 29 (1993) 193–197, https://doi.org/10.1016/0956-716x(93)90307-e.
- [11] C.S. Goh, J. Wei, L.C. Lee, M. Gupta, Properties and deformation behaviour of Mg-Y2O3 nanocomposites, Acta Mater. 55 (2007) 5115–5121, https://doi.org/ 10.1016/j.actamat.2007.05.032.
- [12] W. Mirihanage, W. Xu, J. Tamayo-Ariztondo, D. Eskin, M. Garcia-Fernandez, P. Srirangam, P. Lee, Synchrotron radiographic studies of ultrasonic melt processing of metal matrix nano composites, Mater. Lett. 164 (2016) 484–487, https://doi.org/10.1016/j.matlet.2015.11.022.
- [13] M. Habibnejad-Korayem, R. Mahmudi, W.J. Poole, Enhanced properties of Mg-based nano-composites reinforced with Al2O3 nano-particles, Mater. Sci. Eng. A 519 (2009) 198–203. https://doi.org/10.1016/j.msea.2009.05.001.
- [14] R.K. Davies, V. Randle, G.J. Marshall, Continuous recrystallization related phenomena in a commercial Al-Fe-Si alloy, Acta Mater. 46 (1998) 6021–6032, https://doi.org/10.1016/S1359-6454(98)00286-9.

- [15] C.S. Kim, I. Sohn, M. Nezafati, J.B. Ferguson, B.F. Schultz, Z. Bajestani-Gohari, P. K. Rohatgi, K. Cho, Prediction models for the yield strength of particle-reinforced unimodal pure magnesium (Mg) metal matrix nanocomposites (MMNCs), J. Mater. Sci. 48 (2013) 4191–4204, https://doi.org/10.1007/s10853-013-7232-x.
- [16] W. Xu, A. Maksymenko, S. Hasan, J.J. Meléndez, E. Olevsky, Effect of external electric field on diffusivity and flash sintering of 8YSZ: a molecular dynamics study, Acta Mater. 206 (2021), 116596, https://doi.org/10.1016/j. actamat. 2020.116596
- [17] W. Xu, K. Ramirez, S. Gomez, R. Lee, S. Hasan, A bimodal microstructure for fatigue resistant metals by molecular dynamics simulations, Comput. Mater. Sci. 160 (2019) 352–359, https://doi.org/10.1016/j.commatsci.2019.01.026.
- [18] W. Xu, A.P. Horsfield, D. Wearing, P.D. Lee, Classical and quantum calculations of the temperature dependence of the free energy of argon, Comput. Mater. Sci. 144 (2018) 36–41, https://doi.org/10.1016/j.commatsci.2017.12.001.
- [19] W. Xu, A.P. Horsfield, D. Wearing, P.D. Lee, First-principles calculation of Mg/MgO interfacial free energies, J. Alloy. Compd. 650 (2015) 228–238, https://doi.org/ 10.1016/j.jallcom.2015.07.289.
- [20] D. Wearing, A.P. Horsfield, W. Xu, P.D. Lee, Which wets TiB2 inoculant particles: Al or Al3Ti, J. Alloy. Compd. 664 (2016) 460–468, https://doi.org/10.1016/j. islance 2015 13 202
- [21] M.S. Hasan, R. Lee, W. Xu, Deformation nanomechanics and dislocation quantification at the atomic scale in nanocrystalline magnesium, J. Magnes. Alloy 8 (2020) 1296–1303, https://doi.org/10.1016/j.jma.2020.08.014.
- [22] A. Kardani, A. Montazeri, Metal-matrix nanocomposites under compressive loading: towards an understanding of how twinning formation can enhance their plastic deformation, Sci. Rep. 10 (2020), https://doi.org/10.1038/s41598-020-6696-1.
- [23] H.-T. Chung, D.-S. Cheong, C.-S. Kim, Role of nanoparticle in {PNN}-{PZT}/Ag nanocomposite, Mater. Lett. 59 (2005) 920–924, https://doi.org/10.1016/j.matlet.2004.01.042.
- [24] H. Lu, F. Liang, J. Gou, Nanopaper enabled shape-memory nanocomposite with vertically aligned nickel nanostrand: controlled synthesis and electrical actuation, Soft Matter 7 (2011) 7416, https://doi.org/10.1039/c1sm05765k.
- [25] P. Hirel, Atomsk: a tool for manipulating and converting atomic data files, Comput. Phys. Commun. 197 (2015) 212–219, https://doi.org/10.1016/j.cpc.2015.07.012.

- [26] A. Mazahery, M.O. Shabani, Mechanical properties of A356 matrix composites reinforced with nano-SiC particles, Strength Mater. 44 (2012) 686–692, https://doi.org/10.1007/s11223-012-9423-0.
- [27] Y. Mishin, D. Farkas, M.J. Mehl, D.A. Papaconstantopoulos, Interatomic potentials for monoatomic metals from experimental data and ab initio calculations, Phys. Rev. B - Condens. Matter Mater. Phys. 59 (1999) 3393–3407, https://doi.org/ 10.1103/PhysPayR 50.3303
- [28] T. Brink, Tersoff-style three-body potential for SiC developed by Tersoff (1989) v002, (2019). doi:10.25950/5E8E8324.
- [29] C.R. Dandekar, Y.C. Shin, Molecular dynamics based cohesive zone law for describing Al-SiC interface mechanics, Compos. Part A Appl. Sci. Manuf. 42 (2011) 355–363, https://doi.org/10.1016/j.compositesa.2010.12.005.
- [30] A.P. Thompson, H.M. Aktulga, R. Berger, D.S. Bolintineanu, W.M. Brown, P. S. Crozier, P.J. in 't Veld, A. Kohlmeyer, S.G. Moore, T.D. Nguyen, R. Shan, M. J. Stevens, J. Tranchida, C. Trott, S.J. Plimpton, LAMMPS a flexible simulation tool for particle-based materials modeling at the atomic, meso, and continuum scales, Comput. Phys. Commun. 271 (2022), 108171, https://doi.org/10.1016/j.cpc.2021.108171.
- [31] A. Stukowski, Visualization and analysis of atomistic simulation data with OVITO the open visualization tool, Model. Simul. Mater. Sci. Eng. 18 (2010), 015012, https://doi.org/10.1088/0965-0393/18/1/015012.
- [32] A. Stukowski, Structure identification methods for atomistic simulations of crystalline materials, Model. Simul. Mater. Sci. Eng. 20 (2012), https://doi.org/ 10.1088/0965-0393/20/4/045021, 45021-15.
- [33] A. Stukowski, K. Albe, Extracting dislocations and non-dislocation crystal defects from atomistic simulation data, Model. Simul. Mater. Sci. Eng. 18 (2010), 085001, https://doi.org/10.1088/0965-0393/18/8/085001.
- [34] M.A. Tschopp, D.E. Spearot, D.L. McDowell, Atomistic simulations of homogeneous dislocation nucleation in single crystal copper, Model. Simul. Mater. Sci. Eng. 15 (2007) 693–709, https://doi.org/10.1088/0965-0393/15/7/001.
- [35] X.L. Zhong, W.L.E. Wong, M. Gupta, Enhancing strength and ductility of magnesium by integrating it with aluminum nanoparticles, Acta Mater. 55 (2007) 6338–6344, https://doi.org/10.1016/j.actamat.2007.07.039.
- [36] L. Ceschini, A. Dahle, M. Gupta, A.E.W. Jarfors, S. Jayalakshmi, A. Morri, F. Rotundo, S. Toschi, R.A. Singh, Aluminum and Magnesium Metal Matrix Nanocomposites, Springer, Singapore, 2017, https://doi.org/10.1007/978-981-10-2681-2.